



# Bio-Based Epoxy Resins of Epoxidized Soybean oil Cured with Salicylic acid Loaded with Chitosan: Evaluation of Physical–Chemical Properties

N. C. Nepomuceno<sup>1</sup> · M. V. L. Fook<sup>1</sup> · A. Ries<sup>2</sup> · A. Mija<sup>3</sup> · R. M. R. Wellen<sup>1,4</sup>

Accepted: 5 September 2022 / Published online: 3 January 2023

© The Author(s), under exclusive licence to Springer Science+Business Media, LLC, part of Springer Nature 2023

## Abstract

In this work epoxidized soybean oil (ESO) based compounds were developed using salicylic acid (SAL) and 1, 3, and 5 wt% of chitosan (CHT). The chemical structures and the curing mechanisms were evaluated using Fourier transformed infrared spectroscopy (FTIR). The thermal curing in the absence of catalyst was followed using differential scanning calorimetry (DSC). The data show that ESO/SAL/CHT formulations with low CHT content, i.e. 1 and 3% reacted and with high reactions enthalpy. The obtained bio-resins were characterized by their water uptake, swelling ratio, crosslink density, thermal stability. These results present a new alternative for the development of bio resins based on epoxidized soybean oil, salicylic acid and chitosan, enabling potential applications such as curatives or composite materials.

**Keywords** Bio-compounds · Epoxidized soybean oil · Salicylic acid · Chitosan · Curing

## Introduction

Due to increasing demand for polymers-based materials that are directly linked to ecological problems of low life circle and high levels of waste, the development and implementation of a sustainable economy grounded on renewable resources has triggered great interest from the research community and industry in the last years [1]. The research challenge is to figure out effective ways of converting bio-renewable resources into fuels and chemicals to design innovative, green and environmentally friendly routes for

the development, recovering and reusing of polymeric materials [2, 3].

Among the renewable sources, the vegetable oils (VO) such as linseed and soybean oils, have attracted much attention due to their low cost, non-toxicity, and large worldwide production [4]. In general, the VO are constituted by triglycerides and fatty acids linked to a glycerol core. The chemical treatments, such as acrylation and epoxidation, are the most important and useful exploration of double bonds functionalization, leading to the production of bio-based monomers and resins able to replace those from fossil sources [5].

Epoxidized soybean oil (ESO) obtained from the soybean oil (SO) epoxidation offers a wide range of advantages, due to the SO commercial availability and its large scale production in Brazil as feedstock. The ESO provides advantages as potential raw material for a variety of industrial applications such as products for the automobile, aerospace, and general goods, for instance [6–8]. The presence of the oxirane groups in ESO enables the direct synthesis of epoxy resin via ring-opening reactions with amino or carboxyl groups containing compounds such as diamines [9, 10], dicarboxylic acids [3, 11, 12] and anhydrides [13, 14]. The use of carboxylic acids as initiators and epoxy curing agents is well established mainly in linseed oil biobased systems and the approach for epoxidized soybean oil is still underexplored [15, 16]. In the

✉ A. Mija  
Alice.MIJA@univ-cotedazur.fr

✉ R. M. R. Wellen  
wellen.renate@gmail.com

<sup>1</sup> Academic Unit of Materials Engineering, Federal University of Campina Grande, Campina Grande 58249-140, Brazil

<sup>2</sup> Multidisciplinary Center for Technological Investigations, National University of Asunción, San Lorenzo University Campus, San Lorenzo 111421, Paraguay

<sup>3</sup> Université Côte d'Azur, Institut de Chimie de Nice, UMR 7272 CNRS, 28 Avenue Valrose Cedex 02, 06108 Nice, France

<sup>4</sup> Materials Engineering Department, Federal University of Paraíba, João Pessoa 58051-900, Brazil

last years, research groups have focused on the reactions mechanisms between aliphatic acids and epoxidized vegetable oils, even so, due to the variety of these compounds, some of the carboxylic acids have not been studied so far, for example the salicylic acid that is characterized as a benzoic acid, but presents a functional -COOH group [3, 8, 17].

Salicylic acid (SAL) is a benzoic acid with an *ortho*-hydroxyl group, being a natural product produced for example from Willow tree. SAL is a safe compound used in the pharmaceutical industry due to its excellent antibacterial, anti-infective and antifungal activities [18]. Moreover, SAL is a key plant to regulate immunity hormones (such as jasmonic acid, ethylene, abscisic acid) and exhibits high potential to control the post-harvest losses of the horticultural crop [19, 20].

Chitosan (CHT) is another example of renewable resource, originated from chitin, the second most abundant natural biopolymer after cellulose. It is a copolymer consisting of  $\beta$ -(1–4)-linked d-glucosamine and *N*-acetyl-d-glucosamine [21]. CHT has many desirable properties including non-toxicity, biodegradability, biocompatibility and it may be obtained from marine shell wastes through a chemical process such as deproteinization, demineralization and discoloration [22]. The hydroxyl and primary amines groups of CHT are proper candidates for epoxy curing since they are reactive and can participate in the curing process through the interaction with epoxide groups [23, 24].

The combination between salicylic acid and chitosan has been widely studied with the main purpose to develop proper packages and increase the fruits' shelf-life [20, 25], protecting them against microorganisms (fungi, bacteria etc.) activity [26].

The aim of this work is to synthesize epoxy resins from totally green monomers and without any catalyst/initiator. Thermoset resins based on ESO were cured with salicylic acid (ESO/SAL) at molar ratio of 1.2; CHT was added at 1, 3, and 5 wt.%. The effects of chitosan in the ESO/SAL curing reactions were investigated using differential scanning calorimetry (DSC) and Fourier transformed infrared spectroscopy (FTIR). The obtained biopolymers were characterized in terms of thermal stability by thermogravimetry analysis (TGA). Moreover, the swelling ratio (in water and toluene), contact angle and gel content assessments were determined. It is worth mentioning, from our knowledge, so far, salicylic acid has never been combined.

without any synthetic modifications in its structure as biobased crosslinker for ESO. Chitosan was used to observe its influence on the curing behavior of the thermoset and aiming a simplified methodology to obtain a fully bio-based epoxy resin.

## Materials and Methods

### Materials

Chitosan (deacetylation degree  $\geq 75\%$  and low molar mass) and salicylic acid (98% purity) were acquired from Sigma Aldrich (São Paulo, Brazil). The epoxidized soybean oil (ESO) with equivalent epoxy weight (EEW) of 238 g/mol and the number of epoxy groups per molecule 4.3 was kindly provided by BBC Química (São Paulo, Brazil). Toluene and acetone (98% of purity) were acquired from Sigma Aldrich (São Paulo, Brazil) and used to determine the swelling ratio and gel content, respectively. All chemicals were used as received without further purification.

### Curing Reaction of Epoxidized Soybean oil With Salicylic Acid (SAL) in Presence of Chitosan (CHT)

SAL was added to ESO (ESO/SAL) at the stoichiometric ratio  $R = 1.2$  epoxy/acid groups, that was chosen based on previous literature work [9, 27–30]. The proper amount of ESO (5 mL) was heated at 80 °C, afterward, SAL (1.21 g) was added, and the compounds were mechanically stirred for 10 min until reaching complete homogenization. CHT at contents 1, 3 and 5 wt.% was added to the uncured ESO/SAL mixture and mechanically stirred for 5 min at 80 °C until complete dispersion. The uncured mixtures were poured out in a silicon mold and cured at 100 °C for 2 h. A schematic pathway is shown in Fig. 1.

### Fourier Transform Infrared Spectroscopy (FTIR)

Specimens were analyzed using the attenuated total reflectance (ATR) method using a spectrometer Spectrum 400 Series Perkin Elmer (United States) in the range of 400–4000  $\text{cm}^{-1}$  wavenumbers. The resolution and the number of scanning cycles were 16  $\text{cm}^{-1}$  and 32 scans, respectively.

### Differential Scanning Calorimetry (DSC)

Curing of ESO/SAL/CHT mixtures took place using the DSC of TA Instruments model Q20. Specimens weighing 7–9 mg of ESO/SAL and ESO/SAL/CHT (1, 3 and 5 wt.%) were sealed in aluminum pans and heated from 25 °C to 270 °C at a heating rate of 10 °C  $\text{min}^{-1}$ , under inert atmosphere of nitrogen ( $\text{N}_2$ ) with gas flow of 50 mL  $\text{min}^{-1}$ .

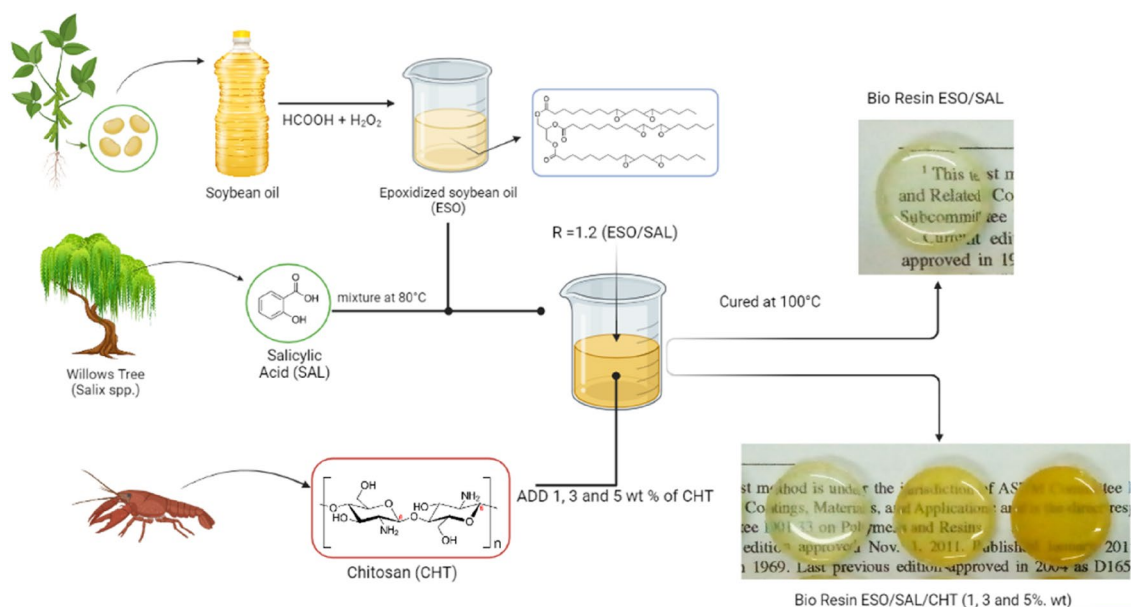


**Fig. 1** Flowchart illustrating how ESO/SAL/CHT bio-resins were obtained

## Thermogravimetry (TGA)

The thermal stability of raw materials (ESO and CHT) and cured ESO/SAL and ESO/SAL/CHT (1, 3 and 5 wt.%) were evaluated using a THA Pyris-1 of Perkin Elmer (United States). Specimens with approximately 10 mg were placed in an alumina pan and heated from room temperature ( $\sim 23\text{ }^{\circ}\text{C}$ ) to  $650\text{ }^{\circ}\text{C}$ , with a heating rate of  $10\text{ }^{\circ}\text{C}\cdot\text{min}^{-1}$ , under inert nitrogen ( $\text{N}_2$ ) atmosphere with gas flow of  $50\text{ mL}\cdot\text{min}^{-1}$ .

## Gel Content (GC)

Gel content is an important parameter that indicates the degree of conversion during the synthesis of any kind of resins and it is calculated using Eq. (1). The cured specimens ( $M_i$ ) were embedded in a filter paper and refluxed in acetone using a Soxhlet apparatus for 48 h. Afterward, the specimens were dried for 6 h until reaching a constant weight ( $M_f$ ).

$$\text{Gel content (\%)} = \frac{(M_i)}{(M_f)} \times 100 \quad (1)$$

## In vitro Hydrolytic Degradation

During the in vitro hydrolytic degradation, the initial specimens ( $W_i$ ) were immersed in a phosphate-buffered saline (PBS) solution (pH 7.4) at  $37\text{ }^{\circ}\text{C}$  for predetermined periods of time, i.e.,  $t=7, 14, 21$  and  $28$  days. Afterward, the

specimens were removed from the solution, washed with distilled water, and dried at  $50\text{ }^{\circ}\text{C}$  until constant weight. The specimens were then weighted ( $W_t$ ) and the hydrolytic degradation was determined using the Eq. (2).

$$\text{Hydrolytic degradation (HD)(\%)} = \frac{W_i - W_t}{W_i} \times 100 \quad (2)$$

where  $W_i$  is the initial weight and  $W_t$  is the weight at a pre-determined time. The experiments were carried out in triplicate.

## Swelling Ratio and Crosslinking Density

The swelling ratio ( $S_r$ ) was determined according to Eq. (3) and the results are shown as absorbed solvent content expressed in percentage unit. The swelling factor ( $S_f$ ) used in Eq. (5) was the unitary value of the swelling ratio.

The tests were performed using toluene as solvent. Specimens with  $1 \pm 0.01\text{ g}$  as the dried weight ( $W_d$ ) and with  $15 \times 15 \times 5.3\text{ mm}^3$  were immersed in 50 mL of toluene for 24 h. Then, the specimens were gently dried to remove solvent excess and the swollen weights ( $W_s$ ) were recorded.

$$\text{Swelling ratio } (S_r \text{ in \%}) = \frac{W_s - W_d}{W_s} \times 100 \quad (3)$$

The swelling ratio in toluene was used to determine the crosslink density ( $\nu_d$ ) and the molar mass between crosslinking points ( $M_c$ ) of prepared resins. According to Flory-Rehner theory [31, 32], the crosslink density can be calculated using the Eq. 4.

$$v_d = \frac{\ln(1 - v_p) + v_p + \chi_1 v_p}{v_s \left( \frac{v_p}{2} - v_p^{\frac{1}{3}} \right)} = \frac{1}{M_c} \quad (4)$$

where  $v_s$  is the solvent molar volume and  $\chi_1$  is the Flory–Huggins polymer–solvent interaction parameter, which for toluene is equal to  $106.27 \text{ cm}^3 \cdot \text{mol}^{-1}$  and  $\sim 0.391$ , respectively. The molar volume of the polymer  $v_p$  can be calculated using Eq. 5.

$$v_p = \frac{\frac{1}{\rho_{\text{polymer}}}}{\frac{S_f}{\rho_{\text{solvent}}} + \frac{1}{\rho_{\text{polymer}}}} \quad (5)$$

where  $\rho_{\text{polymer}}$  and  $\rho_{\text{solvent}}$  are the densities of the polymer (calculated from the relation between mass and volume of specimens) and that of the solvent, while  $S_f$  is the swelling factor.

### Water Absorption (WA)

To determine the percentage of water absorption, the specimens were immersed in distilled water at  $\sim 37^\circ \text{C}$  and weighted at pre-determined immersion times. The water uptake degree was determined according to Eq. 6.

$$\text{Water absorption } (W_a\%) = \frac{W_t - W_d}{W_t} \times 100 \quad (6)$$

where  $W_d$  and  $W_t$  are the weight of dried specimens and after immersion, respectively.

### Contact Angle

Specimens' wettability was analyzed with a contact angle apparatus following the standard ASTM D724 – 99. Specimens with  $5 \times 5 \times 1 \text{ mm}^3$  were placed on a microscope slide and tested with different liquids (PBS pH of 7.4 and distilled water pH of 6.0) through the deposition of 3 drops ( $10 \mu\text{L}$ ) upon the specimen surface. The images were recorded using a DLSR camera Canon T6 and the contact angles were measured with the software SW Angle calculator.

## Results and Discussions

### Curing Mechanism Involving ESO, SAL and CHT

The mechanisms of the reactions among epoxide groups are quite complex and reactions beyond oxirane ring-opening such as esterification, etherification and condensation esterification can occur simultaneously. Based on the acquired data and previous studies [12, 15], three main mechanisms

among epoxide groups and carboxylic acids are illustrated in the Scheme 1a and the proposed interactions with chitosan in Scheme 1b.

### Fourier Transform Infrared Spectroscopy (FTIR)

Figure 2 displays FTIR spectra of uncured mixtures and cured ESO/SAL and ESO/SAL/CHT bio-resins. The ESO spectra showed the main characteristics bands of the epoxide group at  $848$  and  $824 \text{ cm}^{-1}$  and the ester band centered at  $1744 \text{ cm}^{-1}$ . Other bands such as  $728 \text{ cm}^{-1}$  (CH bending),  $1084$ – $1154 \text{ cm}^{-1}$  (ester, antisymmetric stretch), and  $2856$ – $2924 \text{ cm}^{-1}$  (methylene symmetric and antisymmetric stretch) are also observed, they are important to compare the structural changes during the curing [33–35].

The characteristic band due to the oxirane group at  $826 \text{ cm}^{-1}$  decreases along with the crosslinking reaction, and bands at  $3456$ – $3182 \text{ cm}^{-1}$  referring to OH stretch of intermolecular bonding appear mostly due to the oxirane ring opening reactions which is also an indication of esterification reaction [9].

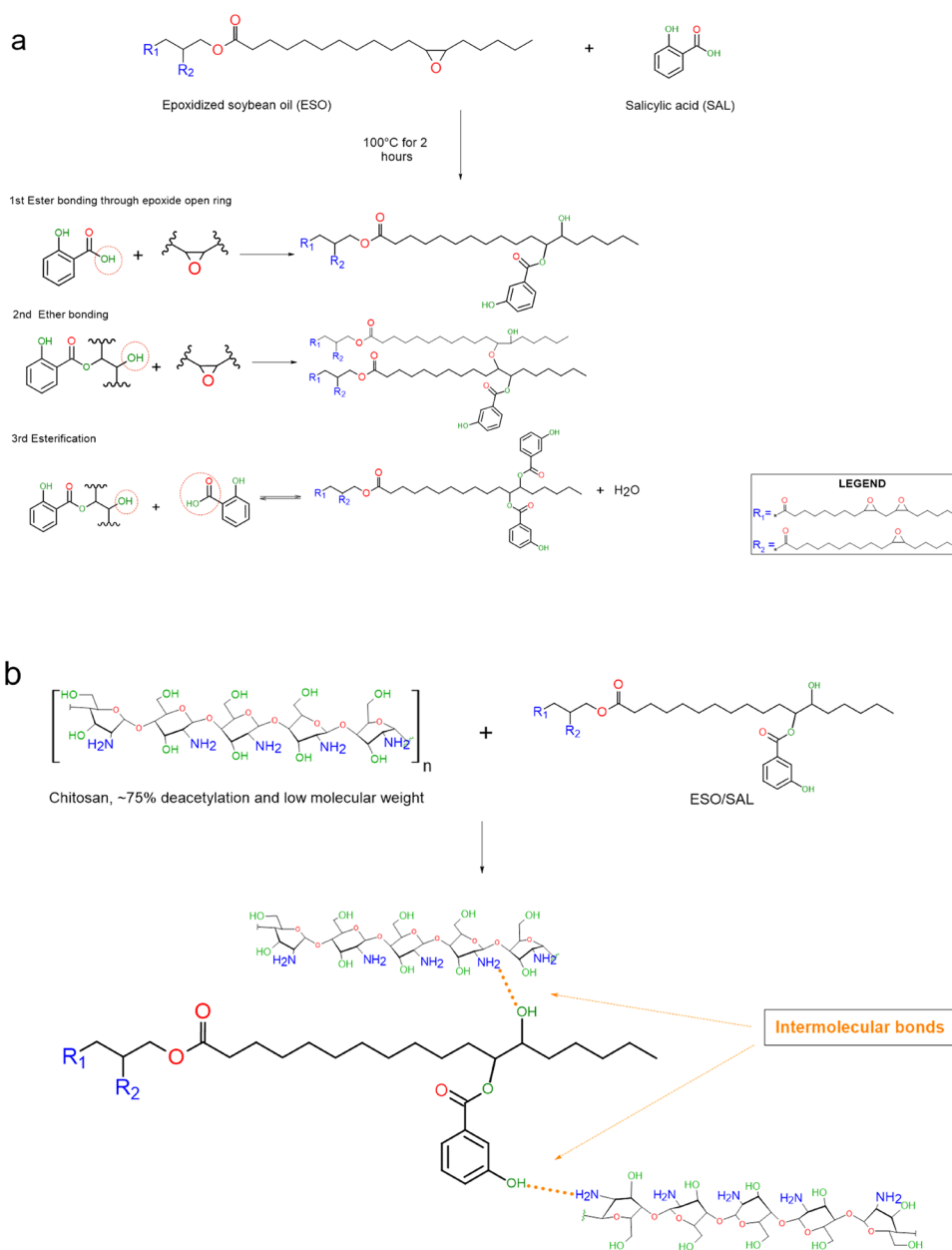
Observing the FTIR spectra of uncured mixtures in the region  $500$ – $1000 \text{ cm}^{-1}$  (Fig. 3-a), can be highlighted that the main peak at  $824 \text{ cm}^{-1}$  of epoxide groups appears in the cured bio-resins slightly divided with another peak occurring at  $\sim 848 \text{ cm}^{-1}$  referring to 1,3 di-substituted benzene positions assumed by OH and COOH groups of SAL which are established at  $874$  and  $806 \text{ cm}^{-1}$  bands for the cured resins. This resonance phenomenon is also demonstrated by the decreasing intensity in the bands of 1,2 di-substituted benzene groups at  $728$  and  $748 \text{ cm}^{-1}$  when the uncured mixtures and cured resins are compared.

The wavenumber interval from  $1000$  to  $1500 \text{ cm}^{-1}$  highlighted in Fig. 3b shows the main characteristic bands which give evidence to the reactions mechanisms proposed in Scheme 1a. The ether CO stretching bands at  $1154$  and  $1028 \text{ cm}^{-1}$  refer to the aliphatic ethers and OH in-plane bending at  $1376 \text{ cm}^{-1}$  indicates the presence of secondary alcohol that is, mainly formed, during the etherification reaction evidencing that the secondary mechanism proposed occurred.

Otherwise, the main mechanism reaction, i.e., ester formation, is evidenced by bands centered at  $1212$  and  $1258 \text{ cm}^{-1}$ , which especially refers to the decrease of aliphatic esters from the ESO structure and the increase of aromatic esters formed due to the SAL presence when uncured and cured compounds are compared. The CH symmetrical and unsymmetrical bending are located at  $1376$ ,  $1458$  and  $1484 \text{ cm}^{-1}$ , respectively, they are another evidence of aromatic benzene compounds linked to the main structure of ESO.

In the interval  $1500$ – $4000 \text{ cm}^{-1}$  (Fig. 2c) may be noticed the band centered at  $1700 \text{ cm}^{-1}$  which refers to the ester

**Scheme 1** Chemical structures of epoxidized soybean oil (ESO) and salicylic acid (SAL) (a); proposed mechanism of reactions between SAL and ESO to obtain bio-resins (b) and the bio-resins with chitosan



group present in ESO and CO stretch of carboxylic groups from SAL, simultaneously. The presence of bands referring to CH aromatic stretch at 3160–3180  $\text{cm}^{-1}$  and the increase of OH intermolecular bonded hydroxyl group between 3200 and 3460  $\text{cm}^{-1}$ , respectively, is a major indication that the opening of the epoxide ring was caused by the presence of SAL's carboxylic groups.

### Differential Scanning Calorimetry (DSC)

DSC scans of fresh mixtures and partially cured ESO/SAL and ESO/SAL/5%CHT bio-resins, at 80 °C for 2 h, are displayed in Fig. 3, and the obtained results are summarized in Table 1. The DSC thermograms of fresh mixtures display

double exothermic peaks (Tpeak 1 and 2), whereas partially cured ESO/SAL displayed only the peak at higher temperatures (Tpeak 2), since partial curing took place during heating at 80 °C for 2 h.

Reactivity information can be extracted based on these DSC scans, the curing at 80 °C suggesting that the salicylic acid is efficient and the first reaction, the main curing reaction, is complete after 2 h. Based on this argument, and considering the chemical structures of compounds used in this work, as well as the Tpeak interval occurring between 100–220 °C, could be suggested that the salicylic acid has higher reactivity than aliphatic carboxylic acids as reported in the literature which presented temperatures between 180–200 °C for the same curing event [27, 36].

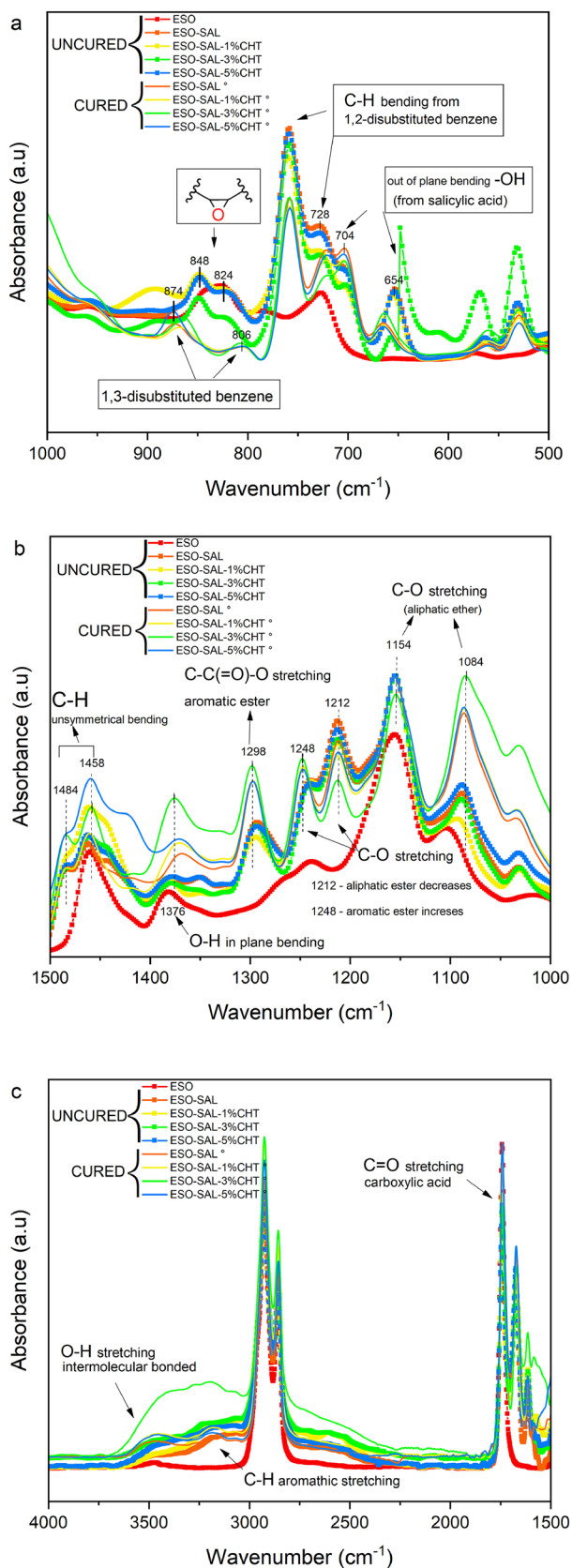


**Fig. 2** FTIR spectra of uncured mixtures and cured resins with the main characteristics peaks highlighted. Zoom in the regions (a) 500–1000  $\text{cm}^{-1}$  (b) 1000–1500  $\text{cm}^{-1}$  and (c) 1500–4000  $\text{cm}^{-1}$

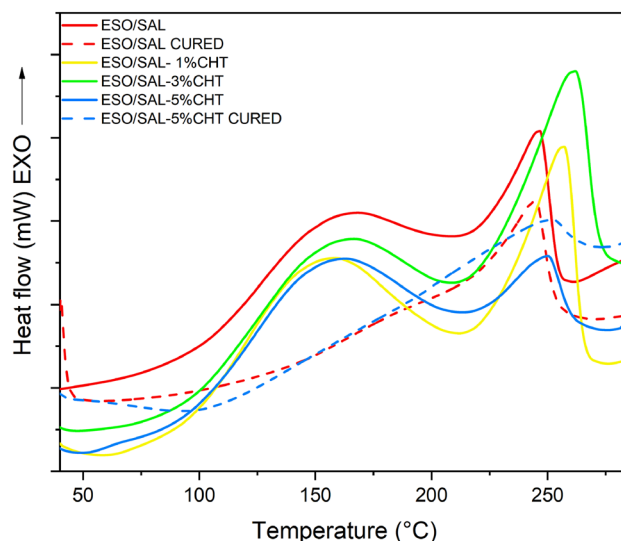


**Fig. 3** DSC scans at 10  $^{\circ}\text{C}/\text{min}$  of uncured ESO/SAL/CHT mixtures and partial cured ESO/SAL and ESO/SAL/5%CHT bio-resins at 80  $^{\circ}\text{C}$  for 2 h

The secondary thermal event (Tpeak 2) takes place between 217–270  $^{\circ}\text{C}$  and it is referred to the homopolymerization or etherification in systems with excess of epoxy which occurs at higher temperatures [37].

Upon chitosan addition, during the first curing event, it is observed a discrete displacement of Tpeak 1 to lower temperatures as also an increase of the enthalpies corresponding to the first and second reactions peaks, which can be due to the presence of higher content of primary amines groups and hydroxyls along with the chitosan macromolecular chains which interacts with reactive groups (i.e. hydroxyl or epoxide groups). These interactions are reported by Satheesh et al. (2014) who evaluated the effect of chitosan as filler in DGEBA/Epoxy curing [38, 39]. Additionally, secondary interactions as hydrogen bonding can improve the ESO/SAL/CHT systems reactivity, as also evidenced by FTIR spectra. An exception on enthalpies values correlation with CHT ratio is the system at 5%CHT which has lower enthalpy of homopolymerization reactions at high temperatures.

Furthermore, the endothermic melting of SAL at around 158  $^{\circ}\text{C}$ , as reported by Ding et al., (2015) does not appear in the DSC scans of Fig. 3, suggesting homogeneous mixtures were produced during formulations preparation.

### Thermogravimetric Analysis (TGA)

The thermal stability of fresh compounds and cured ESO/SAL/CHT bio-resins was investigated using TGA, the thermograms being presented in Fig. 4. Raw materials, i.e. ESO and CHT displayed distinct thermal resistances, related to

**Table 1** Enthalpy ( $\Delta H$ ) and temperature at the maximum of the peaks ( $T_{peak1}$  and 2)

System	$T_{peak1}$ (°C)	$\Delta H(J.g^{-1})$	$T_{peak2}$ (°C)	$\Delta H(J.g^{-1})$
ESO/SAL	164	13	247	31
ESO/SAL CURED	–	–	245	21
ESO/SAL-1%CHT	158	2731	257	41
ESO/SAL-3%CHT	163	2381	262	60
ESO/SAL-5%CHT	157	35	250	13
ESO/SAL5%CHT CURED	–	–	252	7

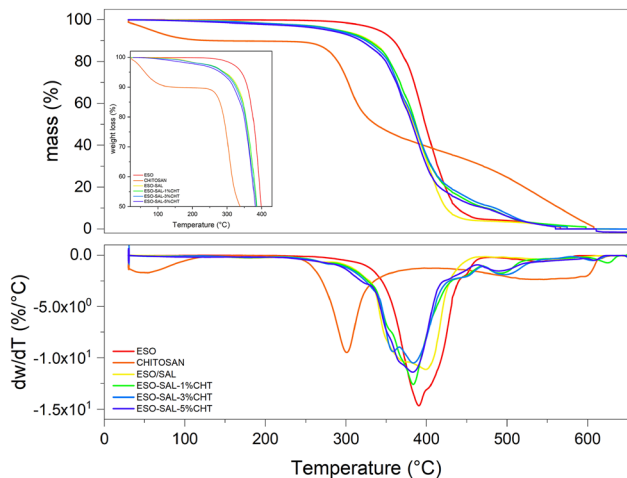


**Fig.4** TG and DTG plots of investigated initial compounds and cured bio-resins, during heating at 10 °C/min

their chemical structures. ESO presents an initial thermal decomposition at ( $T_i$ ) 290 °C and a maximum decomposition ( $T_{max}$ ) at 395 °C which is attributed to the ester groups degradation [10]. The chitosan starts to lose mass at around 100 °C due to the moisture loss followed by its major degradation step at  $T_i$  250 °C,  $T_{max}$  at 350 °C, the mass residue at 600 °C being of 0.25%. The thermal stability of chitosan is inversely proportional to the deacetylation degree (DD) and molecular weight, respectively, the  $NH_2$  groups being less stable than N-acetyl groups [40, 41]. Since the used chitosan presents DD ~ 75% and low molecular weight, these results are expected.

Related to the cured bio-resins,  $T_{max}$  of thermal pyrolysis can be observed between 370–395 °C. A second mass loss at 480 °C can be observed for ESO/SAL/CHT, which can be due to CHT.

**In vitro Hydrolytic Degradation**

Figure 5 presents the evolution of hydrolytic degradation of ESO/SAL/CHT bio-resins carried out in PBS (pH=7.2, 0.01 M), at 37 °C during 7, 14, 21 and 28 days. It can be observed that the bio-resins have low percentages of hydrolytic degradation at the end of the immersing period of

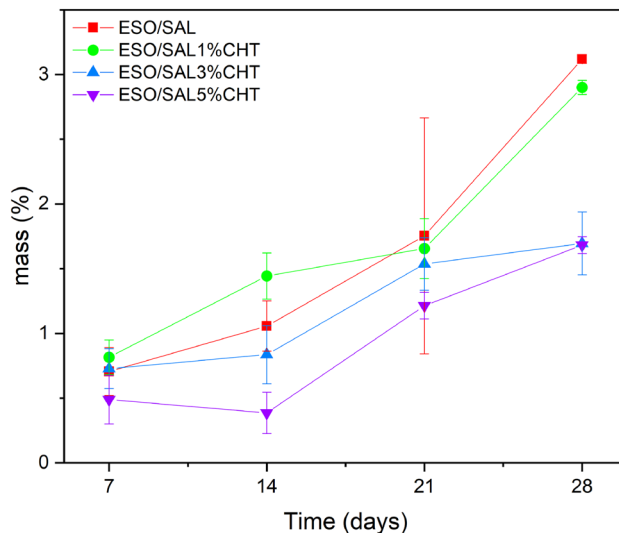


**Fig. 5** Hydrolytic degradation in PBS solution of ESO/SAL/CHT bio-resins

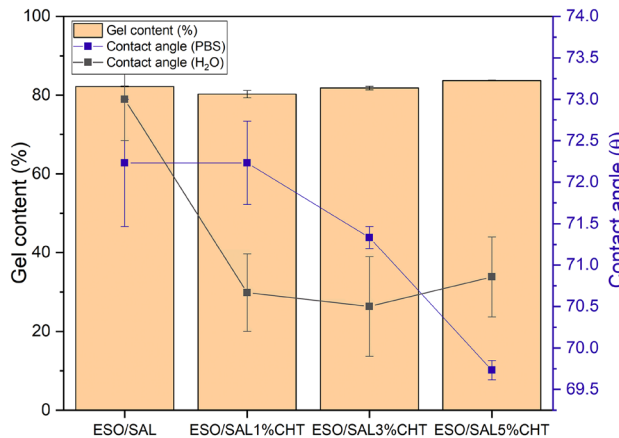


**Fig. 6** Gel content (GC) (black line) and Contact angle ( $\theta$ ) (purple line) of investigated bio-resins (Color figure online)

around  $3 \pm 0.2\%$  for ESO/SAL while for ESO/SAL/CHT bio-resins the obtained values are around 1.5%. This degradation profile shows the contribution of CHT to generate a more stable crosslinked structure, which needs higher energy and/

or longer times to degrade in the tested conditions. These results are comparable with those reported by Wang et al. 2012 for ESO cured with an amine, which presented hydro catalytic degradation values around 1.5%. Fig. 6

### Gel Content (GC) and Contact Angle

GC data obtained applying Eq. (1) for the ESO/SAL/CHT bio-resins are shown in Fig. 7. CHT addition did not show a significant change in GC; hence ESO/SAL and ESO/SAL/CTH present similar values, around  $80 \pm 2\%$  which suggests the existence of similar crosslinked networks. This result can be due to the used stoichiometric ratio ( $R = 1.2$  epoxide/COOH) and to the good reactivity of ESO and SAL together

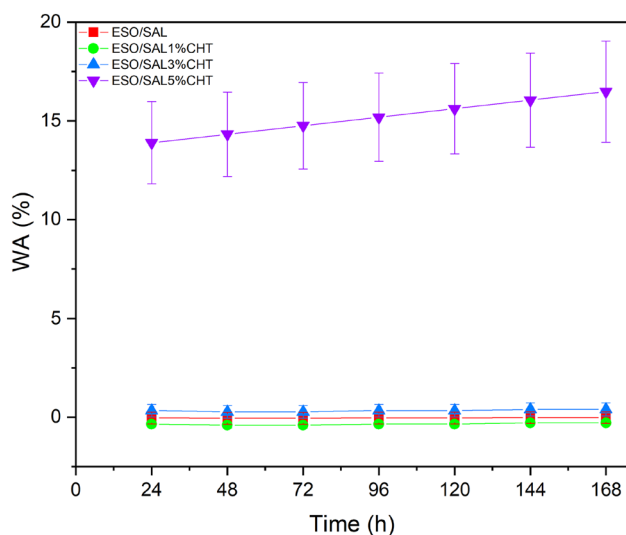
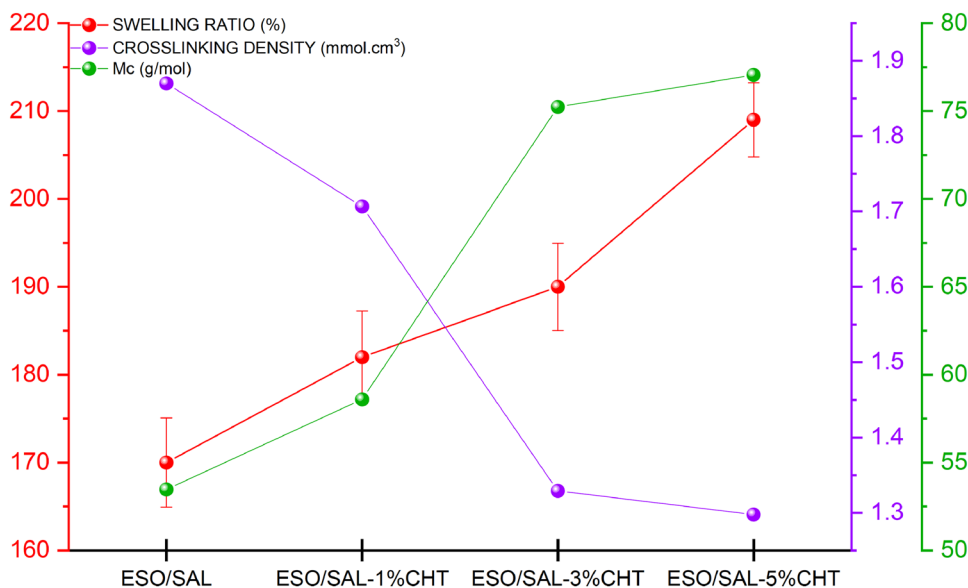


Fig. 7 Water uptake of ESO/SAL with 1, 3 and 5 wt.% of chitosan

Fig. 8 Influence of chitosan content (1, 3 and 5 wt.% CHT) in the swelling ratio in toluene, crosslink density and molar mass between crosslink points ( $M_c$ ) of ESO/SAL/CHT bio-resins



with very good chemical compatibility of the CHT with the epoxy system.

Observing the contact angle values in H<sub>2</sub>O and PBS solutions may be verified that the ESO/SAL and ESO/SAL/1%CHT are mostly hydrophobic ( $\theta \sim 70\text{--}120^\circ$ ). The addition of chitosan in the ESO/SAL formulations tends to slightly decrease this hydrophobic character, this trend is observed in the water uptake results in which samples with 5 wt.% chitosan showed a significant water absorption.

### Water Absorption (WA%)

The water uptake of a material is affected by the polarity of its constituents' surface. The results obtained for the prepared bio-resins given in Fig. 7 shows low values of WA%, excepting the ESO/SAL/5%CHT, mostly due to its higher content on ester linkages. Besides the presence of OH groups formed during the reaction, the main aliphatic chain disfavor the interaction with water [13]. The bio-resin with 5% wt. CHT presents higher WA% which can be explained by the high content of CHT providing a structure more susceptible to water permeation. These results are in good agreement with the gel content and contact angle data, previously discussed.

### Swelling Ratio and Crosslinking Density ( $\nu_d$ )

Acquired data for the swelling ratio in toluene correlated with calculated values of the crosslink density ( $\nu_d$ ) and molar mass of segment chains between crosslinks ( $M_c$ ) are presented in Fig. 8. It may be noticed that the bio-resins swelling is increasing with the CHT addition, this trend is expected when nonpolar solvents such as toluene are used and demonstrates the solvents capacity to permeate into the



bio-resins microstructure and inducing the macromolecular chains displacement without breaking the primary bonds, in other words, “specimens swell, but do not dissolve, in good solvents” [42].

The swelling results are indicating that the chitosan participates during the curing process of the bio-resins, providing a greater distance between the chains and consequently facilitating the solvent penetration. The obtained swelling results were used to estimate the crosslink density and the molar mass between crosslinks ( $M_c$ ) through the theory described by Flory-Rehner [31, 32]. The results show that ESO/SAL and ESO/SAL/CTH bio-resins have similar values of crosslinking density to those reported for ESO/ dicarboxylic acids bio-resins, where values between 1.3 and 1.9 were gathered [11]. It is worth mentioning that chitosan addition drastically decreased the crosslink density which confirms the interactions between ESO/SAL bio-resins and chitosan at intermolecular levels. The calculated values of the molar mass between crosslink points ( $M_c$ ) also indicate an increase of the segments with the CHT addition, a sign that the CHT is contributing to the crosslinking reaction.

## Conclusions

Epoxidized soybean oil-based compounds were prepared using salicylic acid and the addition of 1, 3 and 5 wt.% of chitosan and their influence on the curing mechanism and physico-chemical properties were evaluated. During the curing, ether and ester bonding were evidenced through FTIR spectra. The curing took place during heating and from DSC scans two exothermal events were obtained, the lower one related to the main curing reaction, while the higher one could be related to the homopolymerization. ESO/SAL/CTH formulations with 1 and 3% of CHT reacted faster, with higher reaction enthalpy than that with 5% wt. CHT. In the last system, a higher content of secondary interactions as hydrogen bonding is suggested by FTIR spectra. The gel content and contact angle show that the addition of chitosan in the ESO/SAL formulations tends to slightly decrease the hydrophobic character, mainly when 5% wt. of chitosan is added. The results obtained in swelling ratio in toluene and approaches by Flory-Rehner theory also suggests that ESO/SAL/5% wt. CHT provided a low crosslinked density structure promoting a higher hydrophilic character with intensified swellable character. Gathered data indicates the proper use of produced compounds in curatives and bio-composites.

**Acknowledgements** The author would to thank BBC Química – São Paulo, Brazil for kindly providing the epoxidized soybean oil (ESO)

**Author Contributions** Investigation: NCN. Methodology: NCN, RMRW. Writing of original draft: NCN, AM, RMRW. Supervision: NCN, AM, MVLF, AR, RMRW. Project administration: W, RMR.

**Funding** The authors are grateful to CNPq (National Council for Scientific and Technological Development, Brasília/DF, Brazil) for the financial support. Fundação de Apoio à Pesquisa do Estado da Paraíba (FAPESQ) (Concession term: 017/2019). Professor Renate Wellen is CNPq fellow (no: 307488/2018–7). Conselho Nacional de Desenvolvimento Científico e Tecnológico, 140635/2019–0, Neymara Cavalcante Nepomuceno, 307488/2018–7, Renate Maria Ramos Wellen, Fundação de Apoio à Pesquisa do Estado da Paraíba, 017/2019, Renate Maria Ramos Wellen

**Data Availability** The datasets generated during and/or analysed during the current study are available from the corresponding author on reasonable request.

## Declarations

**Conflict of interest** There is no conflict of interest and all authors have agreed with this submission and they are aware of the content.

## References

- Gandini A, Lacerda TM, Carvalho AJF, Trovatti E (2016) Progress of Polymers from Renewable Resources: Furans, Vegetable Oils, and Polysaccharides. *Chem Rev* 116:1637–1669. <https://doi.org/10.1021/acs.chemrev.5b00264>
- Gandini A (2008) Polymers from Renewable Resources: A Challenge for the Future of Macromolecular Materials. *Macromolecules* 41:9491–9504. <https://doi.org/10.1021/ma801735u>
- Waig Fang S, De Caro P, Pennarun PY et al (2013) Synthesis and characterization of new polyesters based on renewable resources. *Ind Crops Prod* 43:398–404. <https://doi.org/10.1016/j.indcrop.2012.07.027>
- Ortiz P, Wiekamp M, Vendamme R, Eevers W (2019) Bio-based Epoxy Resins from Biorefinery By-products 14:3200–3209
- Tan SG, Chow WS, Tan SG, Chow WS (2017) Biobased Epoxidized Vegetable Oils and Its Greener Epoxy Blends : A review. *Polym Plast Technol Eng.* <https://doi.org/10.1080/03602559.2010.512338>
- Alarcon RT, Lamb KJ, Bannach G, North M (2021) Opportunities for the Use of Brazilian Biomass to Produce Renewable Chemicals and Materials. *Chemsuschem* 14:169–188. <https://doi.org/10.1002/cssc.202001726>
- Hu F, Yadav SK, La Scala JJ et al (2021) Epoxidized soybean oil modified using fatty acids as tougheners for thermosetting epoxy resins: Part 1. *J Appl Polym Sci* 138:50570. <https://doi.org/10.1002/APP.50570>
- Hu F, La Scala JJ, Yadav SK et al (2021) Epoxidized soybean oil modified using fatty acids as tougheners for thermosetting epoxy resins: Part 2—Effect of curing agent and epoxy molecular weight. *J Appl Polym Sci* 138:50579. <https://doi.org/10.1002/APP.50579>
- Frias CF, Serra AC, Ramalho A et al (2017) Preparation of fully biobased epoxy resins from soybean oil based amine hardeners. *Ind Crops Prod* 109:434–444. <https://doi.org/10.1016/j.indcrop.2017.08.041>
- Wang Z, Zhang X, Wang R et al (2012) Synthesis and characterization of novel soybean-oil-based elastomers with

- favorable processability and tunable properties. *Macromolecules* 45:9010–9019. <https://doi.org/10.1021/ma301938a>
11. Di Mauro C, Malburet S, Genua A et al (2020) Sustainable Series of New Epoxidized Vegetable Oil-Based Thermosets with Chemical Recycling Properties. *Biomacromol* 21:3923–3935. <https://doi.org/10.1021/acs.biomac.0c01059>
  12. Falco G, Sbirrazzuoli N, Mija A (2019) Biomass derived epoxy systems: From reactivity to final properties. *Mater Today Commun.* <https://doi.org/10.1016/j.mtcomm.2019.100683>
  13. Pansumdaeng J, Kuntharin S, Harnchana V, Supanchaiyamat N (2020) Fully bio-based epoxidized soybean oil thermosets for high performance triboelectric nanogenerators. *Green Chem* 22:6912–6921. <https://doi.org/10.1039/d0gc01738h>
  14. Ma S, Liu X, Fan L et al (2014) Synthesis and properties of a bio-based epoxy resin with high epoxy value and low viscosity. *Chemsuschem* 7:555–562. <https://doi.org/10.1002/cssc.201300749>
  15. Tran TN, Di MC, Graillot A, Mija A (2020) Chemical Reactivity and the Influence of Initiators on the Epoxidized Vegetable Oil/Dicarboxylic Acid System. *Macromolecules* 53:2526–2538. <https://doi.org/10.1021/acs.macromol.9b02700>
  16. Ding C, Shuttleworth PS, Makin S et al (2015) New insights into the curing of epoxidized linseed oil with dicarboxylic acids. *Green Chem* 17:4000–4008. <https://doi.org/10.1039/c5gc00912j>
  17. Menager C, Guigo N, Vincent L, Sbirrazzuoli N (2020) Polymerization kinetic pathways of epoxidized linseed oil with aliphatic bio-based dicarboxylic acids. *J Polym Sci* 58:1717–1727. <https://doi.org/10.1002/pol.20200118>
  18. Métraux JP (2002) Recent breakthroughs in the study of salicylic acid biosynthesis. *Trends Plant Sci* 7:332–334
  19. Hu F, Sun T, Xie J et al (2021) Functional properties of chitosan films with conjugated or incorporated salicylic acid. *J Mol Struct.* <https://doi.org/10.1016/j.molstruc.2020.129237>
  20. Molamohammadi H, Pakkish Z, Akhavan HR, Saffari VR (2020) Effect of Salicylic Acid Incorporated Chitosan Coating on Shelf Life Extension of Fresh In-Hull Pistachio Fruit. *Food Bioprocess Technol* 13:121–131. <https://doi.org/10.1007/s11947-019-02383-y>
  21. Renault F, Sancey B, Badot P-M, Crini G (2009) Chitosan for coagulation/flocculation processes – An eco-friendly approach. *Eur Polym J* 45:1337–1348. <https://doi.org/10.1016/J.EURPOLYMJ.2008.12.027>
  22. El KH, Belaabed R, Addaou A et al (2018) Chemical modification and characterization of chitin and chitosan. *Int J Biol Macromol* 120:1181–1189. <https://doi.org/10.1016/j.ijbiomac.2018.08.139>
  23. Crini G (2019) Historical review on chitin and chitosan biopolymers. *Environ Chem Lett* 17:1623–1643
  24. Alves NM, Mano JF (2008) Chitosan derivatives obtained by chemical modifications for biomedical and environmental applications. *Int J Biol Macromol* 43:401–414
  25. Lo'ay AA, Taher MA, (2018) Effectiveness salicylic acid blending in chitosan/PVP biopolymer coating on antioxidant enzyme activities under low storage temperature stress of 'Banati' guava fruit. *Sci Hort (Amsterdam)* 238:343–349. <https://doi.org/10.1016/j.scienta.2018.05.005>
  26. Kumaraswamy RV, Kumari S, Choudhary RC et al (2019) Salicylic acid functionalized chitosan nanoparticle: A sustainable biostimulant for plant. *Int J Biol Macromol* 123:59–69. <https://doi.org/10.1016/j.ijbiomac.2018.10.202>
  27. Gobin M, Loulergue P, Audic JL, Lemiègre L (2015) Synthesis and characterisation of bio-based polyester materials from vegetable oil and short to long chain dicarboxylic acids. *Ind Crops Prod* 70:213–220. <https://doi.org/10.1016/j.indcrop.2015.03.041>
  28. Tang Q, Chen Y, Gao H et al (2019) Bio-Based Epoxy Resin from Epoxidized Soybean Oil. *Soybean Biomass Yield Prod.* <https://doi.org/10.5772/intechopen.81544>
  29. Ma Z, Wang Y, Zhu J et al (2017) Bio-based epoxy vitrimers: Reprocessability, controllable shape memory, and degradability. *J Polym Sci Part A Polym Chem* 55:1790–1799. <https://doi.org/10.1002/pola.28544>
  30. Huang X, Yang X, Liu H et al (2019) Bio-based thermosetting epoxy foams from epoxidized soybean oil and rosin with enhanced properties. *Ind Crops Prod.* <https://doi.org/10.1016/j.indcrop.2019.111540>
  31. Treloar LRG (1975) *The physics of rubber elasticity*
  32. Flory PJ (1953) *Principles of polymer chemistry*. Cornell University Press
  33. Qi M, Xu YJ, Rao WH et al (2018) Epoxidized soybean oil cured with tannic acid for fully bio-based epoxy resin. *RSC Adv* 8:26948–26958. <https://doi.org/10.1039/c8ra03874k>
  34. Zhao S, Wang Z, Kang H et al (2018) Fully bio-based soybean adhesive in situ cross-linked by interactive network skeleton from plant oil-anchored fiber. *Ind Crops Prod* 122:366–374. <https://doi.org/10.1016/j.indcrop.2018.06.013>
  35. Pradhan S, Pandey P, Mohanty S, Nayak SK (2017) Synthesis and characterization of waterborne epoxy derived from epoxidized soybean oil and bioderived C-36 dicarboxylic acid. *J Coatings Technol Res* 14:915–926. <https://doi.org/10.1007/s11998-016-9884-3>
  36. Zeng R, Wu Y, Li Y et al (2017) Curing behavior of epoxidized soybean oil with biobased dicarboxylic acids. *Polym Test* 57:281–287. <https://doi.org/10.1016/j.polymertesting.2016.12.007>
  37. Pin JM, Sbirrazzuoli N, Mija A (2015) From epoxidized linseed oil to bioresin: an overall approach of epoxy/anhydride cross-linking. *Chemsuschem* 8:1232–1243. <https://doi.org/10.1002/cssc.201403262>
  38. Satheesh B, Tshai KY, Warrior NA (2014) Effect of Chitosan Loading on the Morphological, Thermal, and Mechanical Properties of Diglycidyl Ether of Bisphenol A/Hexamethylenediamine Epoxy System. *J Compos* 2014:1–8. <https://doi.org/10.1155/2014/250290>
  39. Shibata M, Fujigasaki J, Enjoji M et al (2018) Amino acid-cured bio-based epoxy resins and their biocomposites with chitin- and chitosan-nanofibers. *Eur Polym J* 98:216–225. <https://doi.org/10.1016/j.eurpolymj.2017.11.024>
  40. Pokhrel S, Lach R, Le HH et al (2016) Fabrication and Characterization of Completely Biodegradable Copolyester-Chitosan Blends: I. Spectrosc Therm Charact Macromol Symp 366:23–34. <https://doi.org/10.1002/masy.201650043>
  41. Hamedi H, Moradi S, Hudson SM, Tonelli AE (2018) Chitosan based hydrogels and their applications for drug delivery in wound dressings : a review. *Carbohydr Polym* 199:445–460. <https://doi.org/10.1016/j.carbpol.2018.06.114>
  42. Montarnal D, Capelot M, Tournilhac F, Leibler L (2011) Silica-like malleable materials from permanent organic networks. *Science* 334(80-):965–968. <https://doi.org/10.1126/science.1212648>

**Publisher's Note** Springer Nature remains neutral with regard to jurisdictional claims in published maps and institutional affiliations.

Springer Nature or its licensor (e.g. a society or other partner) holds exclusive rights to this article under a publishing agreement with the author(s) or other rightsholder(s); author self-archiving of the accepted manuscript version of this article is solely governed by the terms of such publishing agreement and applicable law.